MCB
Journals.ASM.org

The DHX33 RNA Helicase Promotes mRNA Translation Initiation

Yandong Zhang,[b] Jin You,[b] Xingshun Wang,[b] Jason Weber[a]

ICCE Institute, Department of Internal Medicine, Division of Molecular Oncology, Washington University School of Medicine, St. Louis, Missouri, USA[a]; Department of Biology, South University of Science and Technology of China, Shenzhen, Guangdong, People's Republic of China[b]

DEAD/DEAH box RNA helicases play essential roles in numerous RNA metabolic processes, such as mRNA translation, pre-mRNA splicing, ribosome biogenesis, and double-stranded RNA sensing. Herein we show that a recently characterized DEAD/DEAH box RNA helicase, DHX33, promotes mRNA translation initiation. We isolated intact DHX33 protein/RNA complexes in cells and identified several ribosomal proteins, translation factors, and mRNAs. Reduction of DHX33 protein levels markedly reduced polyribosome formation and caused the global inhibition of mRNA translation that was rescued with wild-type DHX33 but not helicase-defective DHX33. Moreover, we observed an accumulation of mRNA complexes with the 80S ribosome in the absence of functional DHX33, consistent with a stalling in initiation, and DHX33 more preferentially promoted structured mRNA translation. We conclude that DHX33 functions to promote elongation-competent 80S ribosome assembly at the late stage of mRNA translation initiation. Our results reveal a newly recognized function of DHX33 in mRNA translation initiation, further solidifying its central role in promoting cell growth and proliferation.

Mammalian cells maintain tight control of global mRNA translation through the production of ribosomes (1, 2); deregulation in mRNA translation is frequently found in human diseases (3–6) and is regarded as one of the many factors contributing to cancer development (7–9).

Most eukaryotic protein translation initiation occurs by an ordered assembly of a preinitiation complex on the 5′ cap of mRNA (10). After mature mRNA is transported into the cytosol, the distinct 5′ cap of mRNA is recognized and bound by a large protein complex comprising eukaryotic initiation factor 4E (eIF4E), eIF4A, and eIF4G as well as poly(A)-binding protein (PABP) (1, 11, 12). These factors coordinately prevent mRNA degradation while priming mRNAs for translation initiation.

The initial step in mRNA translation involves formation of a ternary complex between eIF2-GTP, Met-tRNA interference, and small 40S ribosomal subunits. This process is stimulated by the translation initiation factors eIF1, eIF3, eIF4F, and eIF5 (13). This large complex, termed the 43S preinitiation complex, attaches to the activated 5′ cap of mRNA. Bound RNA helicases are responsible for unwinding various secondary structures in mRNA as the complex scans along the mRNA from the 5′ end to the 3′ end until it finds the initiation codon. The 60S large ribosome subunit then joins with the 40S subunit to form an 80S ribosome under guidance from eIF5B-GTP (2, 13). eIF2-GTP and eIF5B-GTP are then hydrolyzed into their GDP forms to promote the assembly of the functional initiation complex (14). The detailed mechanism of how elongation-competent 80S ribosomes are assembled prior to initiation or what triggers initiation is not well understood.

Mammalian mRNAs often contain highly structured untranslated regions (UTRs) at the 5′ ends of their open reading frame sequences that must be unwound to allow ribosome recruitment and scanning. Not surprisingly, unwinding of secondary structures in the mRNA 5′ UTR involves the activity of specialized RNA helicases (15). eIF4A and DDX3 are common RNA helicases shared between mammals and *Saccharomyces cerevisiae* yeast cells, while DHX29 appears to be a mammal-specific RNA helicase important in unwinding highly structured mRNA sequences (16). In the study described in this report, we identified a new RNA helicase, DHX33, involved in translation initiation.

Human DHX33 belongs to the DEAH box family of ATP-dependent RNA helicases, a large family of proteins thought to be involved in various aspects of RNA metabolism (17). Many of these RNA helicases remain poorly studied. Recently, we and other groups have identified DHX33 to be an important participant in rRNA biogenesis and in mediating inflammasome formation in response to extracellular double-stranded RNA (dsRNA) (18–20). Oncogenic *Ras* alleles and downstream components of the phosphatidylinositol 3-kinase/AKT/mTOR pathway induce DHX33 protein expression, indicating the potential importance for DHX33 in relaying cell growth regulation signals to the translational machinery (21).

We found DHX33 localized in both the cytosol and the nucleus in several established human cancer cell lines. Furthermore, endogenous DHX33 interacted with the monoribosome, eIF3 complex, DDX3, and mRNAs, implying that it may also be involved in processes other than nucleolar ribosome production. Through polysome profiling and mRNA translation studies, we found that wild-type DHX33 promotes mRNA translation initiation in a mechanism that requires its helicase activity. Thus, our data indicate that DHX33 promotes mRNA translation initiation by promoting elongation-competent 80S ribosome assembly.

MATERIALS AND METHODS

Cell culture. T47D and HCC1806 breast cancer cell lines were maintained in RPMI 1640 medium containing 10% fetal bovine serum (FBS), 2 mM

Received 24 March 2015 Returned for modification 12 April 2015
Accepted 15 June 2015
Accepted manuscript posted online 22 June 2015
Citation Zhang Y, You J, Wang X, Weber J. 2015. The DHX33 RNA helicase promotes mRNA translation initiation. Mol Cell Biol 35:2918–2931. doi:10.1128/MCB.00315-15.
Address correspondence to Yandong Zhang, zhangyd@sustc.edu.cn, or Jason Weber, jweber@dom.wustl.edu.

doi:10.1128/MCB.00315-15

L-glutamine, streptomycin, and penicillin. SKBR3, HeLa, BT549, and MDAMB361 cells were maintained in Dulbecco's modified Eagle's medium (DMEM) containing 10% FBS, streptomycin, and penicillin. HEK293T cells were maintained in DMEM with 10% FBS, streptomycin, and penicillin.

Lentivirus production. The sequences of short hairpin RNAs (shRNAs) targeting human DHX33 (shDHX33) are as follows (5′ to 3′): GC TCAATATCTATCGGACCTT for shDHX33 number 1 (#1-shDHX33), CT CGGGAAACTTCCTCTGAAA for #2-shDHX33, GCAATTTCAGACTC TTTGCTT for #3-shDHX33, GCTATCGCAAAGTGATCATTT for #4-shDHX33; and CATTTCCTTTAGAACCCAAAT for #5-shDHX33. A pLKO.1 vector carrying shRNA for a scrambled sequence (shScrambled) was purchased from Addgene. A series of deletion mutants of DHX33 was generated, using a QuikChange site-directed mutagenesis kit (Stratagene), according to the primers designed by Stratagene online software. To produce knockdown virus, HEK293T cells were transfected with pLKO.1-shRNA, pCMV-VSV-G, and pHR8.2ΔR, which were used for virus packaging, by use of the Lipofectamine 2000 reagent (Life Technologies). To produce virus overexpressing DHX33, pLVX-DHX33 (the wild type or a K94R mutant) was cotransfected with pCMV-VSV-G and pHR8.2ΔR into HEK293T cells. Culture supernatants were harvested at 24 h and 48 h after transfection and then centrifuged at 2,000 rpm for 5 min.

Tandem affinity purification and nano-liquid chromatography Fourier transform MS analysis. DHX33 with a 3× FLAG tag and a streptavidin tag was affinity purified from cytosolic lysates of HCC1806 cells. Specifically, cytosolic lysates were first passed through a StrepTactin column. After washing and elution, crude DHX33 complexes were then incubated with anti-FLAG M2 antibody-coated beads and immunopurified. Mass spectrometry (MS) was performed using the system described previously (22). The survey scans (*m/z* 350 to 2,000) were acquired using Fourier transform ion cyclotron resonance MS with a resolution of 100,000 at *m/z* 421.75 and a target value of 500,000. The 10 most intense ions from survey scans were isolated in the ion trap and analyzed after a target value of 10,000 was reached. The MS/MS isolation width was 2.5 Da, and the normalized collision energy using wide band activation was 35%. The electrospray ionization was accomplished with a spray voltage of 2.2 kV without sheath gas.

Immunoblotting and immunoprecipitation. Whole-cell lysates were prepared by incubation with whole-cell lysis buffer that included 0.5% NP-40 and 1% SDS and that was supplemented with Halt protease and phosphatase inhibitors (Sigma). Lysates were cleared by centrifugation, and the protein concentration was tested by a DC assay (Bio-Rad). Lysates were boiled with SDS sample buffer, separated by SDS-PAGE, and transferred to a polyvinylidene difluoride membrane (Millipore). Membranes were blocked in 5% nonfat dry milk plus Tris-buffered saline–Tween 20 (TBS-T; 10 mmol/liter Tris-HCl [pH 7.4], 150 mmol/liter NaCl, 0.1% Tween 20) buffer and incubated with primary antibodies diluted in blocking buffer at 4°C overnight. The blots were washed with TBS-T buffer and incubated with horseradish peroxidase-conjugated secondary antibodies (1:10,000; GE Healthcare) in blocking buffer at room temperature. Immune complexes were visualized with an enhanced chemiluminescence kit (GE Healthcare). Primary antibodies for immunodetection were sourced as follows: antitubulin (goat; Santa Cruz), anti-DHX33 (Novus), anti-GAPDH (Bethyl), anti-FLAG (Sigma), anti-DDX3 (Bethyl), anti-eIF3H and anti-eIF3G (Bethyl), anti-rpL7, anti-rpL26, anti-rpL3, and anti-rpS2 (Santa Cruz), and anti-eIF2A (Cell Signaling)

Polysome profiling. Cells (3×10^6) were treated with 10 μg/ml cycloheximide for 5 min before they were harvested and counted. Cells were then subjected to cytoplasmic ribosome fractionation as described previously using a sucrose density gradient system ranging from 7% to 47% (Teledyne Isco). Fractions were collected, and protein for Western blot analysis was precipitated with 10% trichloroacetic acid (TCA). RNA was isolated from monosome, disome, and polysome fractions using the TRIzol reagent (Life Technologies) according to the manufacturer's specifications. Reverse transcription (RT) reactions were performed using a SuperScript III first-strand synthesis system (Life Technologies) with an oligo(dT) primer. Real-time PCR was performed on a StepOnePlus system using SsoFast EvaGreen supermix (Bio-Rad) to amplify GAPDH (glyceraldehyde-3-phosphate dehydrogenase) and DDX5 from monosome/disome and polysome fractions. The numbers of transcripts per fraction were calculated from a standard curve generated from serial dilutions of a cDNA sample with a known total RNA amount. The GAPDH and DDX5 mRNA distribution per fraction was calculated as a percentage of the total number of transcripts in all collected fractions.

[^{35}S]methionine pulse-chase labeling. Cells were starved in cysteine- and methionine-free medium for 4 h and then pulsed with [^{35}S]methionine (50 μCi/ml)-containing medium for 15 min before being harvested. The cells were lysed, and supernatants were precipitated with trichloroacetic acid at a concentration of 10%. Protein pellets were subsequently dissolved with 1% SDS, and the protein concentration was analyzed. An equal amount of protein lysates (25 μg) was loaded onto an SDS-polyacrylamide gel, and the gel was transferred to a polyvinylidene difluoride membrane for autoradiography and Coomassie blue staining. The samples were then analyzed for radioactivity by liquid scintillation counting. The data presented were normalized on the basis of an equal amount of protein in each sample.

Immunofluorescence. Cells were fixed with 10% formalin–10% methanol. Cells were then incubated with mouse anti-FLAG (Sigma) at a 1:1,000 dilution. Goat anti-mouse fluorescein isothiocyanate-immunoglobulin was applied to facilitate the visualization of FLAG-tagged DHX33 protein (FLAG-DHX33). To mark cell nucleoli, rabbit anti-nucleophosmin (NPM) was used at a dilution of 1:100, followed by incubation with goat anti rabbitrhodamine-immunoglobulin.

Heterokaryon assay. HeLa cells (2×10^5) were seeded onto glass coverslips and transfected with plasmids. NIH 3T3 cells (6×10^5) were seeded onto the HeLa cells at 24 h posttransfection. Cocultures were then incubated for 30 min with cycloheximide (100 μg/ml), followed by incubation with 50% polyethylene glycol 2000 in phosphate-buffered saline for 105 s. Cocultures were incubated with Dulbecco's modified Eagle's medium containing cycloheximide (100 μg/ml) for an additional 4 h. Heterokaryons were fixed and stained with a mouse anti-FLAG antibody, followed by rhodamine X-conjugated anti-mouse immunoglobulin (Pierce). Nuclei were stained with DAPI (4′,6-diamidino-2-phenylindole). Fluorescent signals were detected with a fluorescence microscope.

Bioluminescence imaging. Cells were plated in a 6-well tissue dish and transfected with pGL3-5′-UTR-F-luc-3′-UTR-GAPDH. Twenty-four hours later, the cells were replated in 96-well plates, D-luciferin was added, and the plate was imaged with an IVIS-100 instrument. These cells were also harvested for total RNA extraction and analyzed by RT-PCR for determination of firefly luciferase (F-luc) transcript levels. To analyze firefly luciferase mRNA levels, the following other primers were used: firefly luciferase forward primer 5′-CCCTGGTTCCTGGAACAATT-3′ and firefly luciferase reverse primer 5′-GCAACCCCTTTTTGGAAACG-3′.

Protein-RNA coimmunoprecipitation assays. Cells stably expressing the FLAG-tagged DHX33 were seeded in 10-cm plates at 2×10^6 cells per plate and incubated overnight. Cells were then lysed in polysome lysis buffer. Insoluble material was removed by centrifugation, and lysates were normalized by the protein concentration and incubated with FLAG M2-agarose for 2 h at 4°C with rotation. Immunoprecipitates were then washed 6 times with polysome lysis buffer. A plasmid carrying the sequence for firefly luciferase was spiked in as an internal control. Beads were then divided into portions for immunoblotting and RNA extraction. For RNA extractions, a NucleoSpin RNA II kit (Clontech) was used. The isolated RNA was used as a template for cDNA synthesis using oligo(dT) primers and analyzed by quantitative PCR. The mRNA abundance in each sample was normalized to that of the spiked-in luciferase. For Western blotting, sample buffer was added to the beads, which were analyzed as described above.

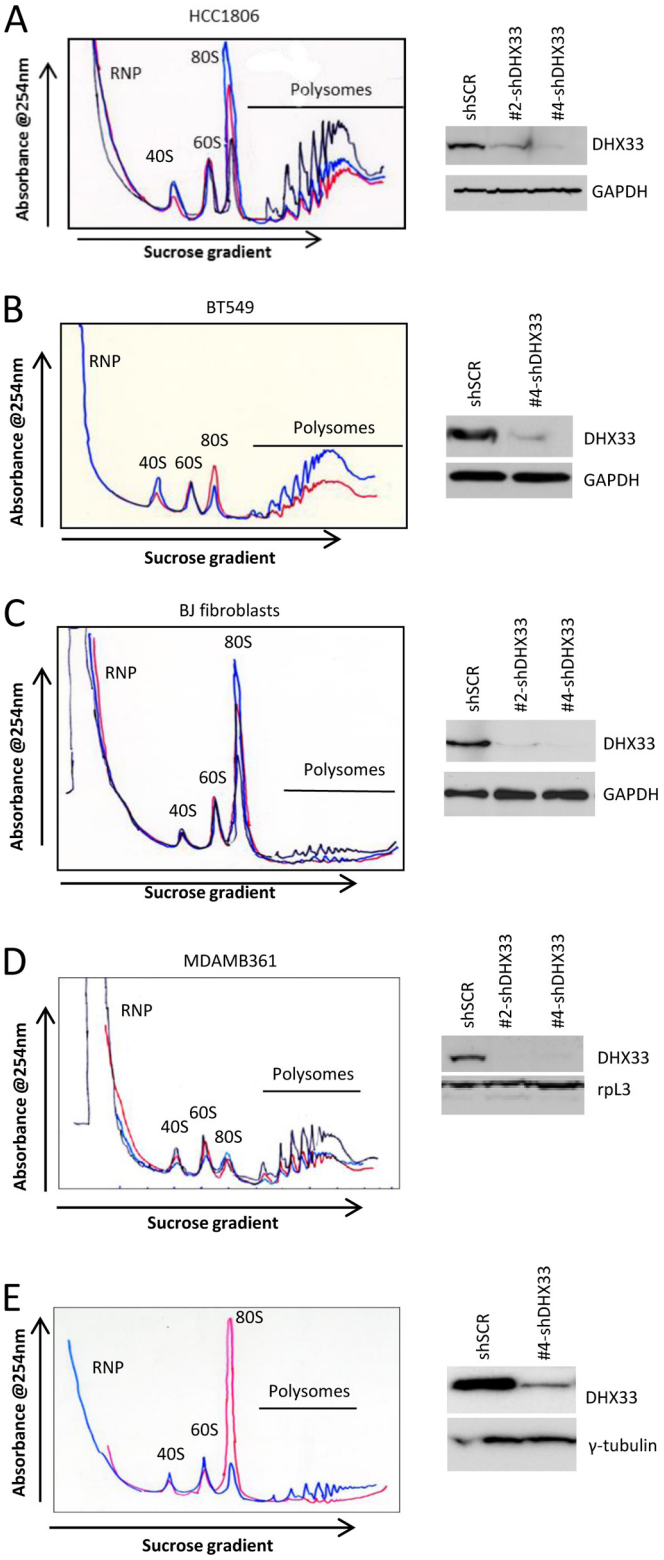

FIG 1 DHX33 knockdown markedly reduces the ratio of polysomes/monosomes. Polysome profiling was performed on HCC1806 cells, BT549 cells, BJ primary fibroblasts, and MDAMB361 cells after lentiviral infection by DHX33-specific shRNA. shScrambled was used as a control. (Left) Polysome profiles; (right) protein knockdown efficiency for each cell line analyzed by Western blotting. Control and knockdown samples were aligned on the basis of the peak position of the 40S ribosome and labeled with distinct colors. (A) Black line, shScrambled (shSCR); red line, #2-shDHX33; blue line, #4-shDHX33. (B) Blue line, shScrambled; red line, #4-shDHX33. (C and D) Black line, shScrambled; red line, #2-shDHX33; blue line, #4-shDHX33. (E) Polysome profiles were determined with 1 M NaCl after HCC1806 cells were infected with lentivirus encoding #2-shDHX33. Blue line, shScrambled; red line, #4-shDHX33.

The following primer sets were used in the PCRs: hGAPDH-FP (5′-CCCACTCCTCCACCTTTGAC-3′) and hGAPDH-BP (5′-CATACCAGGAAATGAGCTTGACAA-3′), hDDX5-FP (5′-ACCAAAACAGGCACAGCATACA-3′) and hDDX5-BP (5′-TACCCCTGGAACGACCTGAA-3′), hDHX8-FP (5′-TAGTAACTTGCTGCGTCTCATACAAA-3′) and hDHX8-BP (5′-GGTCCGAACAGAAGGGTTGTC-3′), hDDX21-FP (5′-CCATGATCTTGCAGTGCTCAA-3′) and hDDX21-BP (5′-GCGGTAGGTACATCAAAGCAAAC-3′), and hUBF-FP (5′-TGACCCCTTATTTCCGCTTC-3′) and hUBF-BP (5′-GTTAGGTCCAGGTTGCTCATC-3′).

RESULTS

DHX33 protein reduction reduces the ratio of polysomes/monosomes in established breast cancer cell lines. We previously identified DHX33 to be a key regulator of nucleolar ribosome biogenesis (20). However, the mechanism behind DHX33's ability to promote cell growth remained unanswered. We sought to determine how DHX33 might integrate with the ribosome machinery to drive mRNA translation. In order to study the requirement for DHX33 in regulating cytosolic ribosome levels and global mRNA translation, we initially performed ribosome profiling following DHX33 knockdown. Breast cancer cell lines BT549, HCC1806, and MDAMB361 and human primary fibroblast BJ cells were each infected with lentiviruses encoding shScrambled as a control and two different shRNAs that target endogenous DHX33. Cells were then subjected to cytosol isolation and continuous ribosome profiling. A reduction in the amount of DHX33 resulted in the accumulation of a significantly larger amount of 80S monoribosomes compared with that obtained with the use of a reduced amount of DHX33, while it markedly inhibited the formation of total polysomes (Fig. 1A to D). There was a significant decrease in the ratio of polysomes/monoribosomes compared to that for the control (Fig. 1A to D). To eliminate the possibility that the 40S and 60S subunits reassociated under low-salt conditions (130 mM KCl), we repeated the ribosome profiling with high-salt buffer (1 M NaCl) after DHX33 knockdown in HCC1806 cells. As shown in Fig. 1E, we observed that DHX33 deficiency again caused 80S ribosomes to accumulate. In all instances, total 80S monoribosome levels were elevated markedly or slightly (Fig. 1A to D). This is in stark contrast to the results of other studies, where the knockdown of ribosome biogenesis proteins resulted in a concomitant reduction in cytosolic 80S ribosome levels (23, 24). Our decreased ratio of polysomes/monoribosomes suggests a significant flaw in translation initiation following DHX33 knockdown (25, 26).

DHX33 promotes protein synthesis through its RNA helicase activity in established cancer cell lines. To determine whether a DHX33 reduction would affect overall protein output, we performed [^{35}S]methionine pulse-label analysis to measure the rate of new total cellular protein synthesis. We introduced five different shRNAs to knock down DHX33 in HCC1806, BT549, and MDAMB361 cells. Equal numbers of cells were pulsed with [^{35}S]methionine to radiolabel newly synthesized proteins, the proteins were extracted, and the incorporation of [^{35}S]methio-

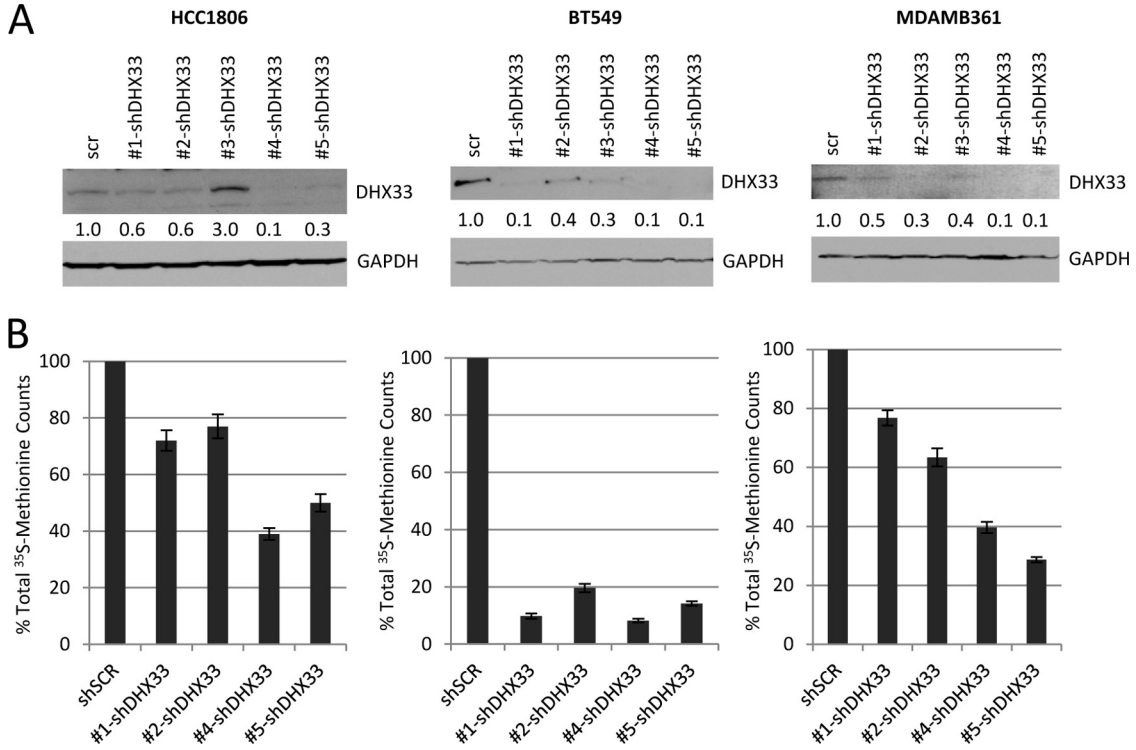

FIG 2 DHX33 is required for new protein synthesis. (A) Five different shRNAs (#1-shDHX33 to #5-shDHX33) were delivered into HCC1806, BT549, and MDAMB361 cells by use of a lentiviral vector. DHX33 protein levels were analyzed by Western blotting to determine the knockdown efficiency. scr, shScrambled. The numbers between the gels are fold changes. (B) A ^{35}S incorporation assay was performed for the above-mentioned cells infected by use of a lentiviral vector; the radioactivity from each sample was analyzed by scintillation counting after normalization for equal total cellular protein levels. Quantitation data are shown. Bars represent the standard deviations from three separate experiments. *P* was <0.005 for all of the DHX33 knockdown samples compared to the results for the shScrambled control.

nine was measured. DHX33 knockdown significantly reduced the level of protein synthesis to various extents in all cell lines tested (Fig. 2).

To determine whether DHX33 RNA helicase activity was required to promote mRNA translation, we performed DHX33 knockdown and rescue experiments. First, we generated a luciferase reporter system to analyze the global protein translational efficiency. Cells were transiently transfected with this firefly luciferase (F-luc) reporter after DHX33 knockdown. F-luc activity was monitored by RT-PCR after normalization of F-luc transcript levels. As shown in Fig. 3A and B, we found that the translational efficiency of mRNA was greatly reduced in DHX33 knockdown cells. We then stably overexpressed an shRNA-resistant wild-type or helicase-dead DHX33 mutant and then knocked down endogenous DHX33 protein levels (Fig. 3C and D). The shRNA-resistant DHX33 was cloned from a mouse. There is 95% similarity and 91% sequence identity between the primary amino acid sequences of mouse DHX33 and human DHX33, and we have previously successfully used it for knockdown rescue assays. Cells were then transfected with firefly luciferase reporter plasmids and analyzed for mRNA translational efficiency. Only the wild-type DHX33 and not the helicase-dead mutant DHX33 was able to rescue the deficiency in mRNA translation (Fig. 3D). Wild-type DHX33 has been shown to function in ribosome biogenesis, making it difficult to determine whether the observed rescue effect was indirectly due to gains in ribosome biogenesis. Thus, we repeated this experiment using a DHX33 mutant lacking residues 1 to 80 (DHX33 Δ1–80, also referred to as the D1 mutant), which is retained in the cytosol and does not partake in nucleolar processes. The N terminus of DHX33 contains a bipartite nuclear localization signal; deletion of this region (residues 1 to 80) causes the D1 mutant to remain in the cytosol (see Fig. 8). As shown in Fig. 3E to G, the D1 mutant of DHX33 was able to markedly rescue the loss of translational activity in cells in which DHX33 was knocked down but failed to rescue the defect in ribosome RNA transcription, as analyzed by determination of 47S pre-rRNA levels. Hence, the separation of DHX33 functions indicated that cytosolic DHX33 promotes protein translation independently of its activity in nucleolar ribosome RNA production.

DHX33 proteins are localized in the cytosol of multiple established cancer cell lines. We have previously shown that DHX33 primarily localizes in the nucleolus of several cell lines. These initial experiments were performed using immunofluorescence to detect endogenous DHX33 in fixed cells. While this technique showed that DHX33 localization was predominantly nucleolar, this technique is hindered by its inability to detect lower levels of proteins in more diffuse subcellular compartments, especially given the strong DHX33 staining of the dense nucleolus. As such, we sought to more accurately measure cytosolic DHX33 using a biochemical analysis. Isolating cytosolic and nuclear subcellular fractions, we were able to detect DHX33 in both subcellular compartments of several established cell lines. As shown in Fig. 4A, HeLa and SKBR3 cells exhibited the largest amount of DHX33 in the cytosol, while T47D cells displayed very little cytosolic

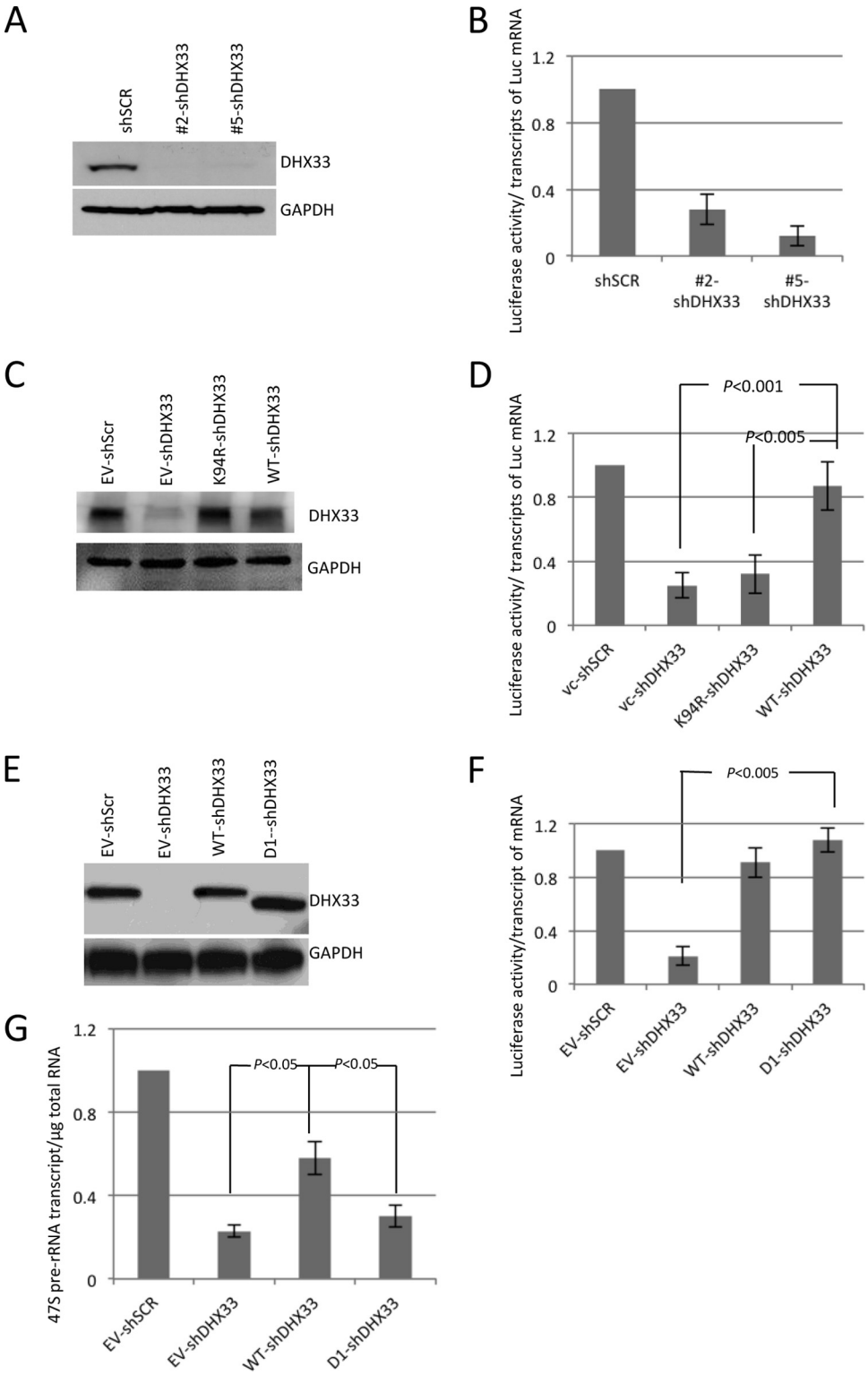

FIG 3 The nucleoside triphosphatase activity of DHX33 promotes mRNA translation. (A) HCC1806 cells were infected with lentiviruses encoding shDHX33or shScrambled (shSCR) as a control. Equal numbers of cells were then transiently transduced with pGL3-5′-UTR-F-luc-3′-UTR-GAPDH. F-luc activity was analyzed by IVIS imaging. Western blot analysis was performed to determine the levels of knockdown of the DHX33 protein. (B) Quantitation data for F-luc activity after normalization of the luciferase transcript levels in each sample. The data shown are the results from three independent experiments, and bars represent standard deviations. *P* was <0.001 for DHX33 knockdown samples compared to the results for the shScrambled control. (C) HCC1806 cells were infected with lentiviruses encoding wild-type (WT) DHX33, the DHX33 K94R mutant, or the empty vector (EV). Cells were then infected with lentiviruses encoding shDHX33 to knock down endogenous DHX33. Western blot analysis was performed to determine the levels of knockdown of the DHX33 protein as well as the level of overexpression of DHX33 (wild-type and K94R mutant DHX33). (D) Equal numbers of cells were then transiently transduced with

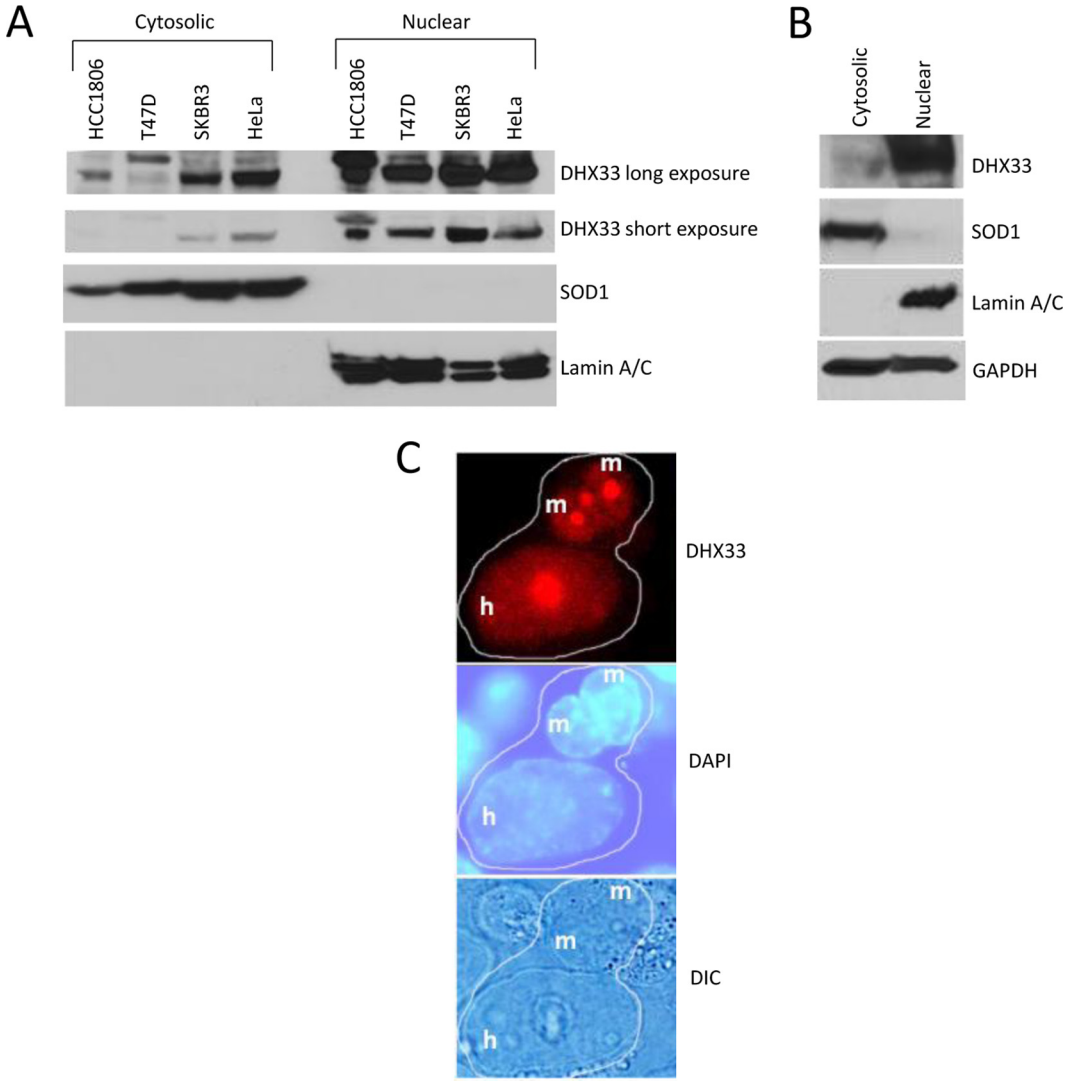

FIG 4 DHX33 participates in nucleolar/cytoplasmic shuttling. (A) T47D, HCC1806, SKBR3, and HeLa cells were fractionated into cytosolic and nuclear fractions, and the DHX33 protein levels in each fraction were analyzed by immunoblotting. SOD1 was used as a cytosolic marker, and lamin A/C was used as a nuclear marker. (B) Human primary fibroblast BJ cells were fractionated into cytosolic and nuclear fractions, and approximately 100 μg each of the cytosolic and nuclear extracts was loaded onto an SDS-polyacrylamide gel for Western blot analysis using antibodies to the indicated proteins. (C) HeLa cells were transiently transfected by pLVX carrying FLAG-tagged wild type-DHX33. At 24 h posttransfection, NIH 3T3 cells were seeded onto these HeLa cells, and the cells were cocultured in the presence of cycloheximide. The cells were then treated with polyethylene glycol to fuse neighboring cells. Indirect immunofluorescence was performed with antibodies recognizing DHX33 to visualize DHX33 protein expression in mouse donor cells (m) and human recipient cells (h). DHX33 staining is red, and the blue DAPI staining demarcates human and mouse nuclei (dominated by heterochromatin). The heterokaryon formed between two mouse cells and a single human cell is outlined in white. DIC, differential interference contrast.

DHX33. We also performed cytosolic and nuclear fractionation on nontransformed BJ primary fibroblasts and analyzed the amounts of DHX33 protein expressed in the cytosolic and nuclear fractions of cells. The DHX33 protein was expressed at levels nearly 50-fold higher in the nucleus than in the cytosol of BJ cells, a nuclear expression/cytosol expression ratio that was much higher than that in HeLa and SKBR3 cancer cell lines (Fig. 4B). The higher cytosolic levels of DHX33 in some cancer cell lines

pGL3-5′-UTR-F-luc-3′-UTR-GAPDH. F-luc activity was analyzed by IVIS imaging. The F-luc activity of each cell sample, after normalization of the F-luc transcript levels, is shown. Data represent the results from three independent experiments, and bars represent standard deviations. (E) HCC1806 cells were infected with lentiviruses encoding wild-type DHX33, the DHX33 Δ1–80 mutant (the D1 mutant), or the empty vector. Cells were then infected with lentiviruses encoding DHX33-specific shRNA to knock down endogenous DHX33. Western blot analysis was performed to determine the levels of knockdown of the DHX33 protein as well as the overexpression of DHX33 (wild-type and mutant D1 DHX33). (F) Equal numbers of cells were then transiently transduced with pGL3-5′-UTR-F-luc-3′-UTR-GAPDH. F-luc activity was analyzed by IVIS imaging. The F-luc activity of each cell sample, after normalization of the F-luc transcript levels, is shown. Data represent the results from three independent experiments, and bars represent standard deviations. (G) Cells were then harvested; total RNA was isolated and analyzed by quantitative RT-PCR for 47S pre-rRNA levels. The bar graph shows 47S rRNA levels after normalization to the amount of total RNA for each sample, and bars represent standard deviations from three independent experiments.

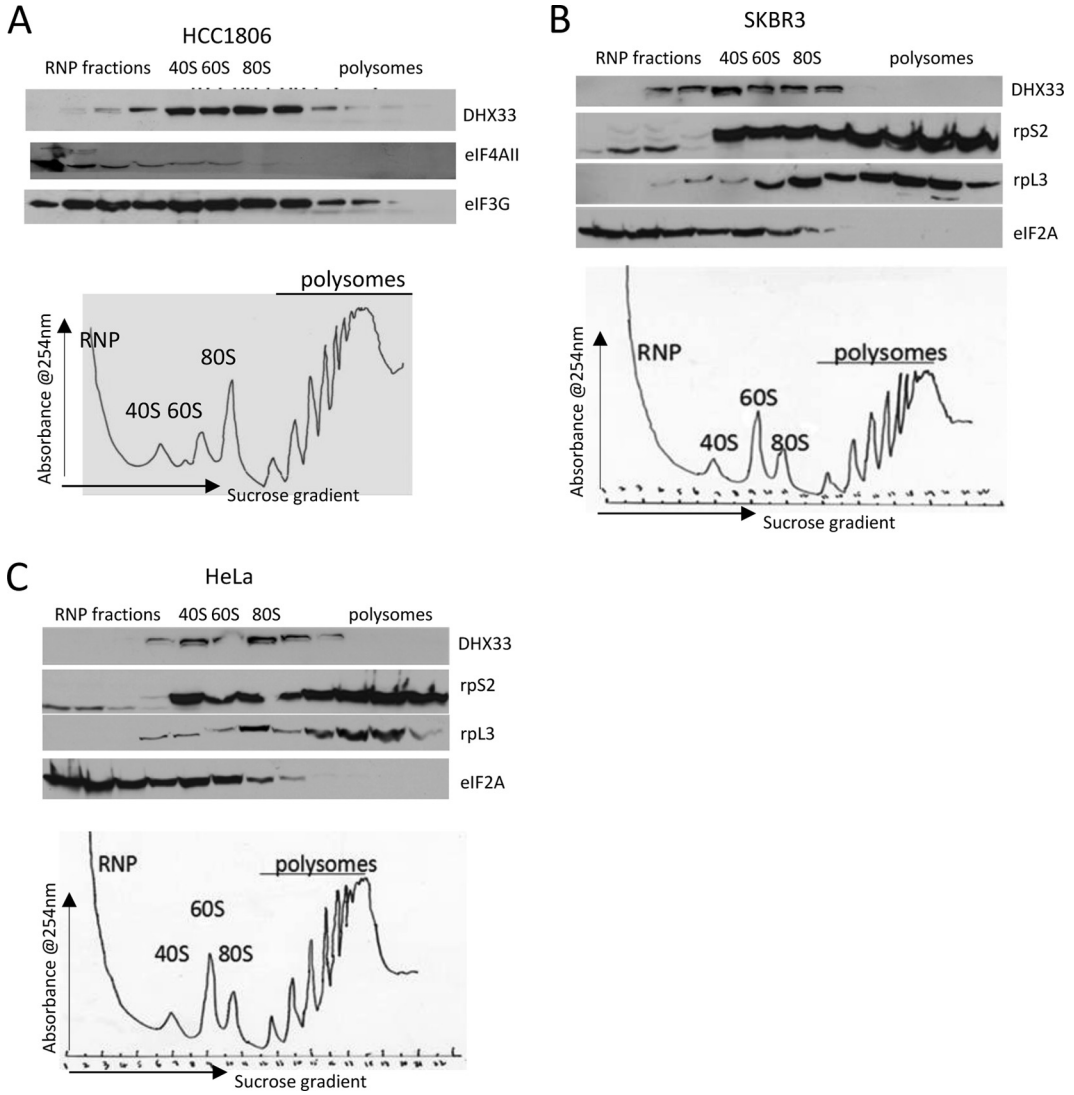

FIG 5 DHX33 cosediments with ribosome subunits and monosomes. Approximately 3×10^6 cells each of HCC1806, SKBR3, and HeLa cells were centrifuged over a sucrose gradient for polysome profiling using a continuous 254-nm monitoring system to detect RNA across the gradient. Fractions were collected and TCA precipitated. Proteins that precipitated from the fractions were analyzed by Western blotting for antibody to each of the indicated proteins.

might indicate that DHX33 contributes to the rapid proliferation of HeLa and SKBR3 cells, although in the case of T47D cells, this localization is not requisite for proliferation. However, these experiments were performed on pools of asynchronously growing cells, where DHX33 localization might be more dynamic than anticipated. Many nucleolar proteins are known to shuttle between the nucleolus and cytosol in a regulated manner. To investigate whether DHX33 participates in this shuttling mechanism, we performed a heterokaryon shuttling assay. DHX33 was first transfected into HeLa cells, NIH 3T3 cells were then seeded onto HeLa cells, and the cells in the mixture of neighboring HeLa and NIH 3T3 cells were fused together by polyethylene glycol in the presence cycloheximide (to prevent the synthesis of new proteins in the recipient NIH 3T3 cells). We were able to visualize the nucleolar localization of DHX33 in NIH 3T3 cells, indicating that DHX33 was able to actively move from the HeLa nucleolus through the NIH 3T3 cytosol and into the NIH 3T3 nucleolus (Fig. 4C).

DHX33 cosediments with monosomes. Having shown a requirement for DHX33 in cytosolic ribosome function, we next sought to determine whether DHX33 associated with cytosolic ribosomes. We performed sucrose gradient fractionations of three established cancer cell lines. This fractionation technique allowed us to identify 40S, 60S, and 80S ribosome subunit and polysome fractions on the basis of continuous monitoring of the sucrose gradient at a wavelength of 254 nm following ultracentrifugation. As shown in Fig. 5, we observed DHX33 expression in fractions that also contained 40S and 60S subunits as well as 80S monosomes. We also probed for the distribution of rpS2 as a marker for the small 40S ribosome subunit protein and rpL3 as a marker for the 60S large ribosome subunit protein, as well as that of eIF2A, eIF4AII, and eIF3G as mRNA translation initiation factors. As expected, eIF2A, eIF4AII, and eIF3G primarily resided in RNP complexes and monosome fractions but not in the heavier polyribosome fractions (Fig. 5). Importantly, the same distribution pattern held true for all three cell lines tested (Fig. 5), indicating

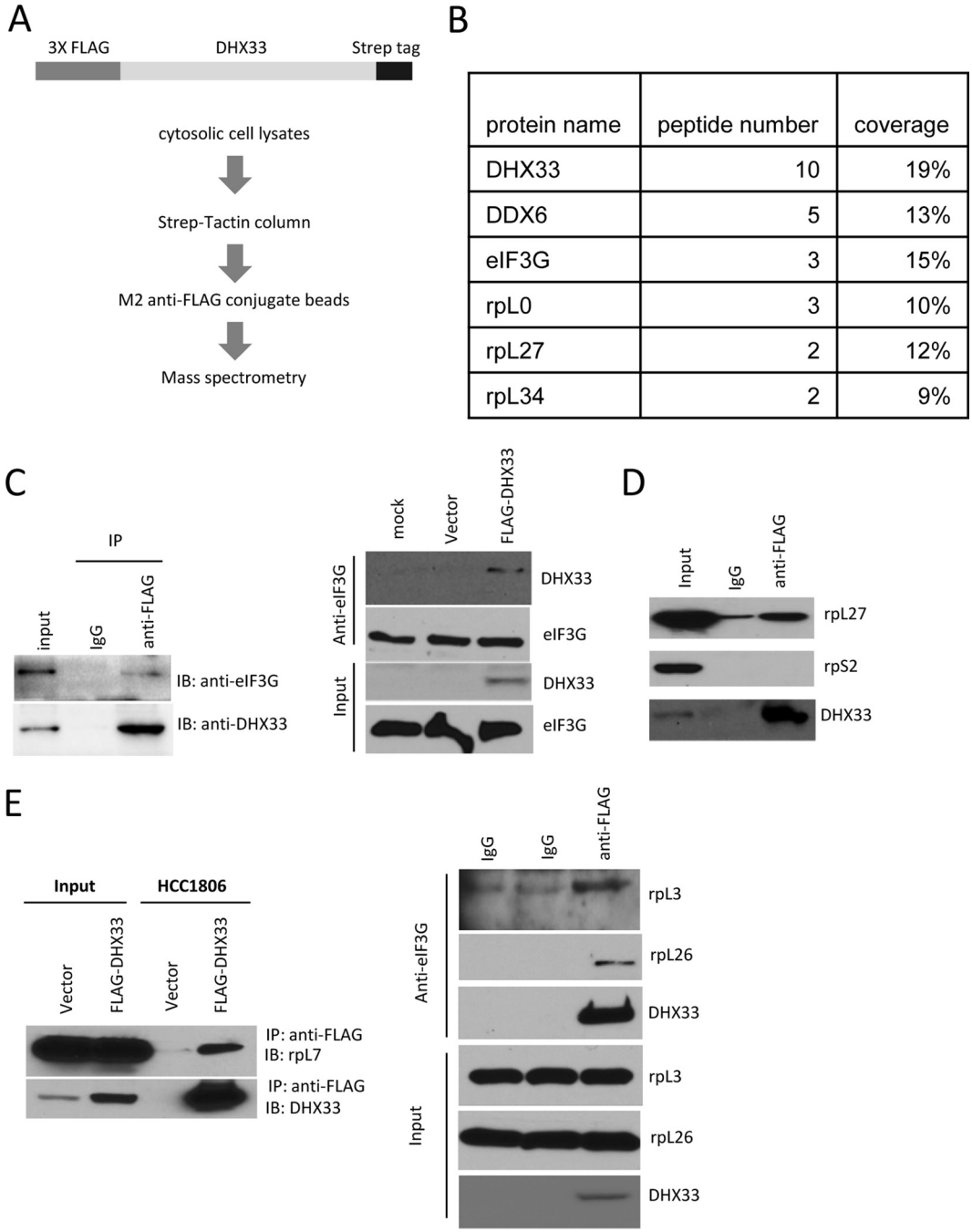

protein name	peptide number	coverage
DHX33	10	19%
DDX6	5	13%
eIF3G	3	15%
rpL0	3	10%
rpL27	2	12%
rpL34	2	9%

FIG 6 DHX33 associates mRNA translation initiation factors and ribosomes. (A) Experimental flowchart for tandem affinity purification of DHX33 from cytosolic extracts doubly tagged with 3× FLAG at the N terminus and streptavidin (Strep) at the C terminus. (B) Proteins identified by MS analysis. Ribosomal proteins and mRNA translation initiation factors were detected in the DHX33 immunoprecipitates. None of these proteins were detected in precipitates from the sample transfected with lentiviruses encoding the empty vector. (C) HCC1806 cells were transduced with pCMV-3×FLAG-DHX33, and cells transfected with lentiviruses encoding the empty vector were used as a negative control. Cell lysates were then immunoprecipitated with anti-eIF3G or anti-FLAG antibodies or with IgG as a control and then immunoblotted with the indicated antibody to detect an association between DHX33 and eIF3G. (D and E) rpL27, rpL7, and rpL26 were found to be coimmunoprecipitated with FLAG-DHX33 in HCC1806 cells. HCC1806 cells were transfected by pCMV-3×FLAG-DHX33; cells transfected with lentiviruses encoding the empty vector were used as a negative control. Cell lysates were then immunoprecipitated with anti-FLAG antibody or with IgG and immunoblotted with antibodies to the indicated proteins. IB, immunoblotting; IP, immunoprecipitation.

that DHX33 associated with individual ribosome subunits and monosomes but not polysomes in the cytosol.

Identification of novel cytosolic DHX33 binding partners. In an effort to identify cytosolic components of a DHX33 protein complex, we constructed a double-tagged DHX33 for affinity purification. In this setting, we engineered DHX33 with an N-terminal triple FLAG epitope tag and a C-terminal streptavidin tag (Fig. 6A). Mass spectrometry was performed to identify DHX33 inter-

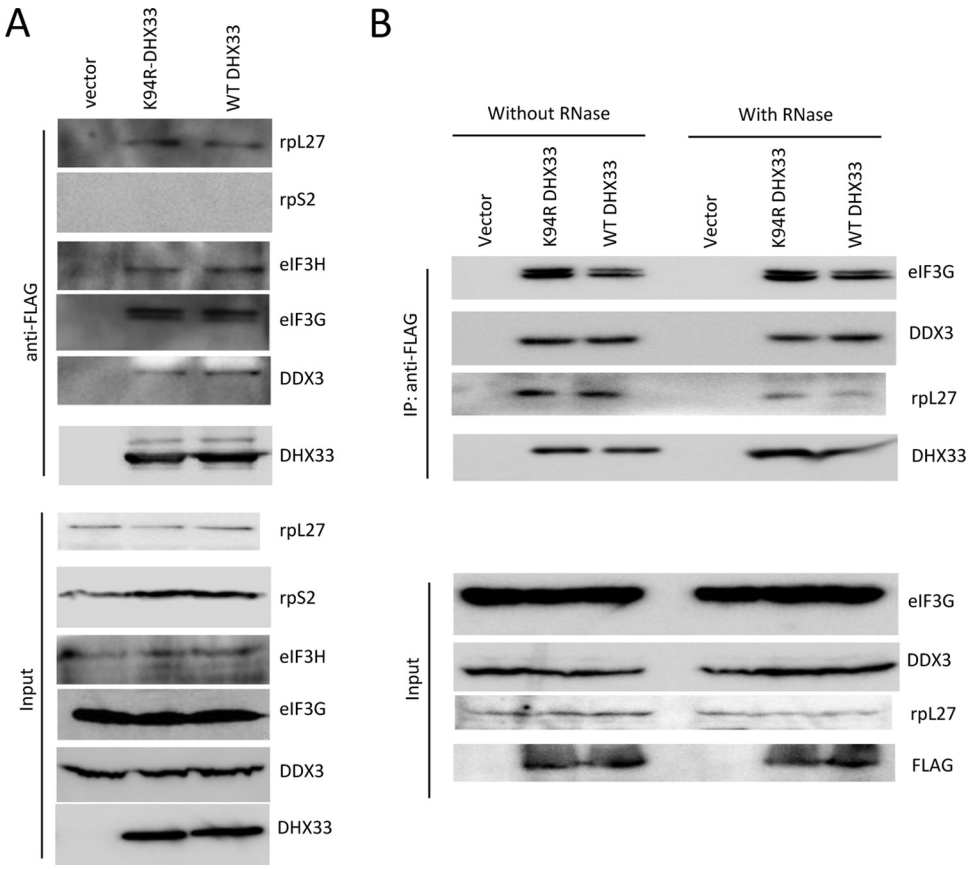

FIG 7 DHX33 helicase activity and RNA interactions are dispensable for DHX33 complex formation. (A) HCC1806 cells were transduced with pCMV-3×FLAG-DHX33 (carrying wild-type or K94R helicase-dead mutant DHX33) and the empty vector as a control. Cell lysates were then immunoprecipitated using an anti-FLAG antibody and immunoblotted with antibodies to the indicated proteins. (B) HCC1806 cells were transduced with pCMV-3×FLAG-DHX33 (wild-type or K94R mutant DHX33) and the empty vector as a control. Cell lysates were then immunoprecipitated by anti-FLAG antibody with 10 μg/ml RNase and without 10 μg/ml RNase and immunoblotted with antibodies to the indicated proteins.

action partners after tandem affinity purification from BT549 cells and by use of the empty vector as a negative control. As shown in Fig. 6B, an array of protein factors involved in mRNA translation was associated with DHX33, but none was associated with the sample transfected with lentiviruses encoding the empty vector as a control. These proteins included translation initiation factor eIF3G and several large ribosomal subunit proteins. Reciprocal immunoprecipitation was performed to verify the interaction between eIF3G and DHX33 (Fig. 6C). We implemented further co-immunoprecipitation experiments using a FLAG epitope antibody and found that DHX33 readily interacted with large ribosome subunit proteins rpL27, rpL26, and rpL7 but did not associate with rpS2 (Fig. 6D and E).

We showed earlier that the DHX33 K94R mutant is unable to rescue the loss of DHX33 in terms of global mRNA translation restoration (Fig. 3). We hypothesized that this defective DHX33 mutant might also be unable to interact with proteins required for translation. However, when we immunoprecipitated the FLAG-tagged DHX33 K94R mutant (20), we found that equal amounts of ribosomal proteins and initiation factors bound to DHX33 K94R and wild-type DHX33 (Fig. 7A). These proteins included eIF3H, eIF3G, DDX3, and rPL27. These findings imply that the helicase activity of DHX33 is not an important factor in regulating the binding between DHX33 and components of the mRNA translation machinery. We further performed the coimmunoprecipitations with and without RNase to examine whether the interaction between DHX33 and the translation machinery was dependent on the existence of RNAs. Treatment with RNase showed that the interaction of DHX33 with DDX3 and eIF3H occurred independently of RNA (Fig. 7B).

DHX33 requires the HA2 domain for binding to eIF3G and requires HA2 and helicase C domains for binding to rpL26. To further delineate the interaction domains between DHX33 and the protein translation factors, a series of DHX33 deletion mutants was constructed (Fig. 8A). The subcellular localization of each DHX33 deletion mutant was examined by immunofluorescence (Fig. 8B). The N-terminal domain of DHX33 contains a nuclear localization signal, and the DHX33 mutant that was expressed diffusely in the cytosol was that in which the nuclear localization signal was deleted (Fig. 8B). Cells were transiently transduced with the DHX33 deletion mutants, and the interaction of DHX33 with eIF3G and rpL26 was determined by coimmunoprecipitation analysis. We found that the formation of DHX33-eIF3G complexes required the HA2 (helicase-associated 2) domain of DHX33 (Fig. 8C), while the DHX33-rpL26 complex required both helicase C and the HA2 domain (Fig. 8D).

DHX33 interacts with mRNAs and promotes translation initiation of the 80S ribosome. Our earlier results indicated a re-

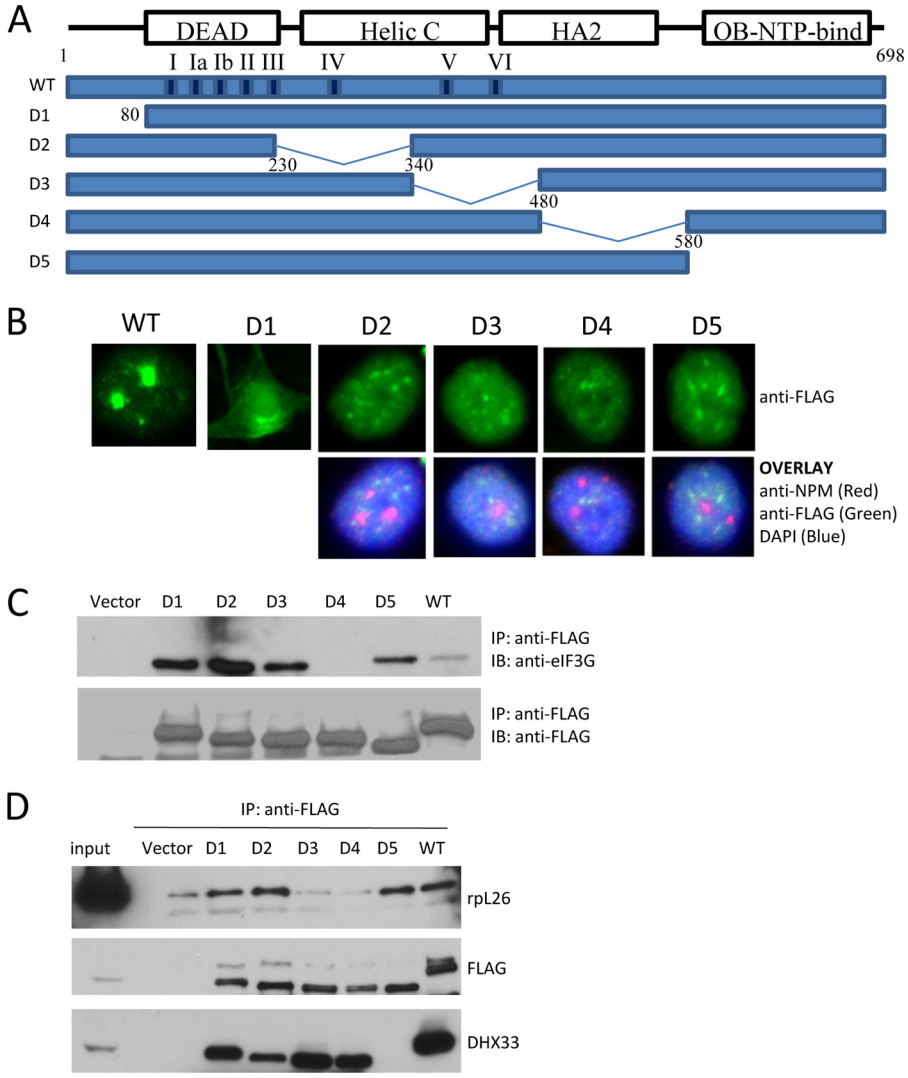

FIG 8 DHX33 binds to eIF3G and ribosomal proteins through shared protein domains. (A) A series of deletion mutants of DHX33 was generated. Diagrams of the sequences of a panel of deletion mutants compared to the sequence of wild-type DHX33 are shown. Helic C, helicase C; OB-NTP-bind, oligonucleotide/oligosaccharide-nucleoside triphosphate binding. (B) HCC1806 cells were transduced with pCMV-3×FLAG-DHX33 carrying the DHX33 wild type and deletion mutants, and cells transduced with the empty vector were used as a control. Cells were then fixed and incubated with anti-FLAG antibody for immunofluorescence detection of mutant DHX33. Anti-NPM was used to mark nucleoli, and DAPI was used to mark nuclei. (C and D) Coimmunoprecipitations were performed using the deletion mutants after transient transduction of each mutant into HCC1806 cells. (C and D) Initiation factor eIF3G required DHX33 residues 480 to 580 (C), while rpL26 required DHX33 residues 340 to 580 (D).

quirement for DHX33 in global mRNA translation (Fig. 2). Moreover, these findings were reinforced by our data showing the formation of cytosolic complexes containing DHX33 and numerous ribosomal proteins and initiation factors and that these complexes cosedimented with 80S monosomes. We next investigated whether cytosolic DHX33 associated with mRNAs using protein-RNA coimmunoprecipitation assays. HCC1806 cells were infected with lentiviruses encoding either an empty vector or 3× FLAG-DHX33. Cytosolic cell lysates were then immunoprecipitated by anti-FLAG antibody, and total RNA was extracted from the immunoprecipitated complexes (Fig. 9A and B). This technique allowed us to identify and enrich several mRNAs that were bound to DHX33. We chose to perform RT-PCRs on a select number of mRNA transcripts with the primer sets indicated above. These mRNAs included *GAPDH*, *DDX21*, *DDX5*, *UBF*, and *DHX8* mRNAs. The GAPDH gene is a housekeeping gene, while DDX21, DDX5, upstream binding factor (UBF), and DHX8 are all known regulators of ribosome biogenesis or mRNA translation. We discovered a significant enrichment of these mRNAs with cytosolic DHX33 irrespective of the length of their 5′ UTRs (Fig. 9C), suggesting that the length of the 5′ UTR is not a factor determining its association with DHX33.

To gain a deeper understanding of the role of DHX33 in the translation of any one specific mRNA, the steady-state distribution of GAPDH mRNA, which we found bound to DHX33, was analyzed by polysome profiling after DHX33 knockdown (Fig. 9D). GAPDH mRNA is efficiently translated and is readily found in the heavy polysome fractions. As shown in Fig. 9E, in cells infected with virus encoding shScrambled it was found that >98% of total GAPDH mRNA was associated with polysomes and about

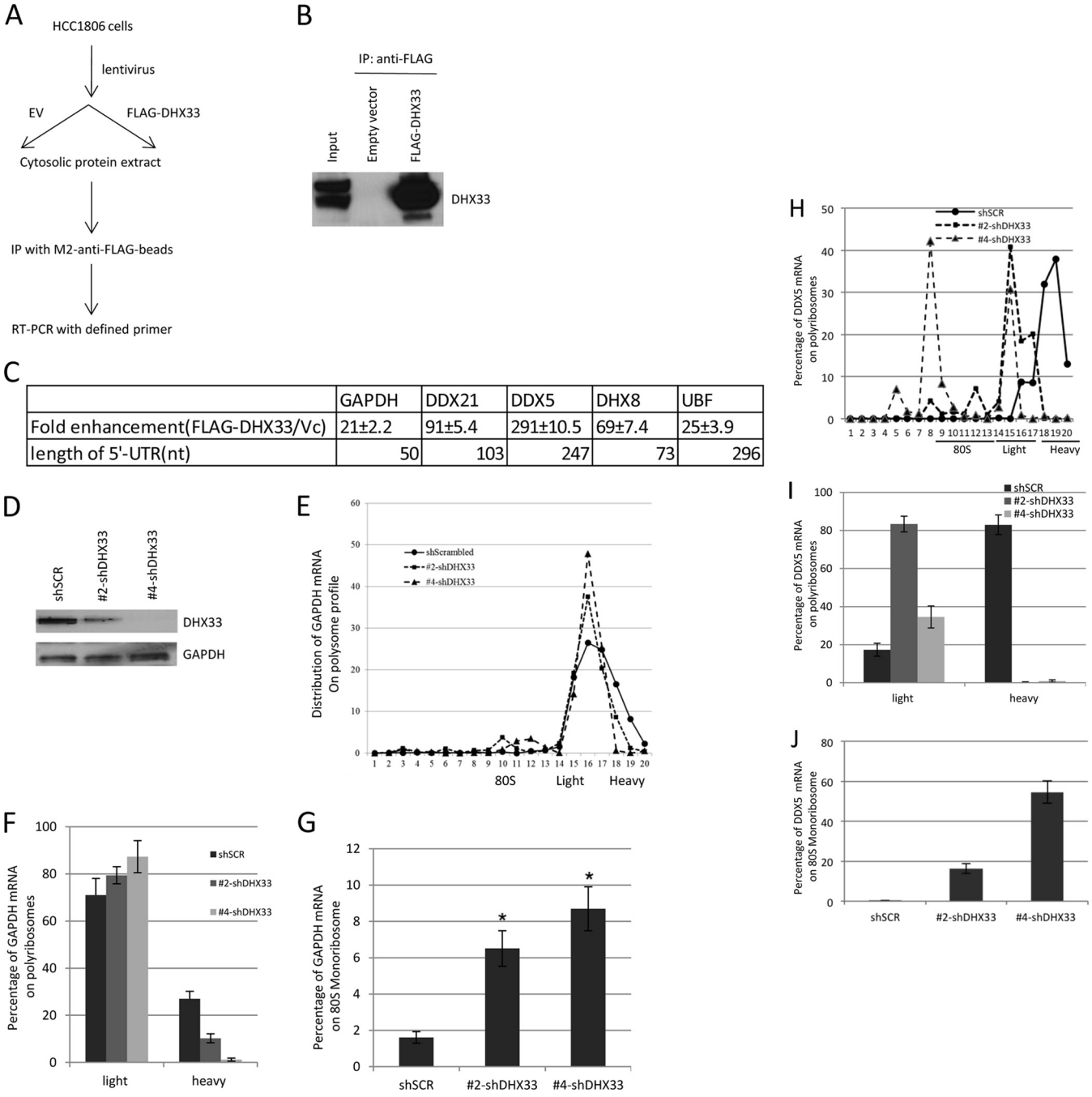

	GAPDH	DDX21	DDX5	DHX8	UBF
Fold enhancement(FLAG-DHX33/Vc)	21±2.2	91±5.4	291±10.5	69±7.4	25±3.9
length of 5'-UTR(nt)	50	103	247	73	296

FIG 9 DHX33 interacts with numerous mRNAs and promotes translation initiation after 80S ribosome assembly. (A) Experimental flowchart describing the immunoprecipitation of DHX33 and analysis of its interacting mRNAs. (B) The immunoprecipitated complex was immunoblotted with anti-DHX33 to confirm that DHX33 is pulled down from cell lysates. (C) FLAG-DHX33 was immunoprecipitated with anti-FLAG antibody, followed by RNA extraction from the immunoprecipitated complex. Quantitative RT-PCR was performed with a primer set defined for each indicated mRNA with the empty vector control (Vc) or DHX33 sample. The data listed are the mean results from three separate experiments, and standard errors are shown. nt, number of nucleotides. (D) HCC1806 cells were infected with lentiviruses encoding shScrambled or DHX33-specific shRNA. The efficiency of knockdown of the DHX33 protein was analyzed by Western blotting with GAPDH as an internal control. (E) Equal cell numbers from the above-mentioned samples were then treated and used for polysome profiling. Fractions from the polysome profiles were collected, and total RNA was extracted from each fraction. These RNA samples were then converted into cDNA and used as the templates for analysis of the GAPDH mRNA distribution. The experiment was repeated three times, and a representative distribution pattern for GAPDH mRNA is shown. (F) Quantitation data from three independent experiments show that DHX33 knockdown redistributes GAPDH mRNA from heavy polysomes to light polysomes ($P < 0.001$; $n = 3$). (G) Quantitation data from three independent experiments show that DHX33 knockdown causes the accumulation of GAPDH mRNA in 80S monosomes (*, $P < 0.005$; $n = 3$). (H to J) Experiments similar to those described above were performed to analyze the polysome distribution of DDX5 mRNA after DHX33 knockdown. The numbers on the *x* axis in panel H are fraction numbers.

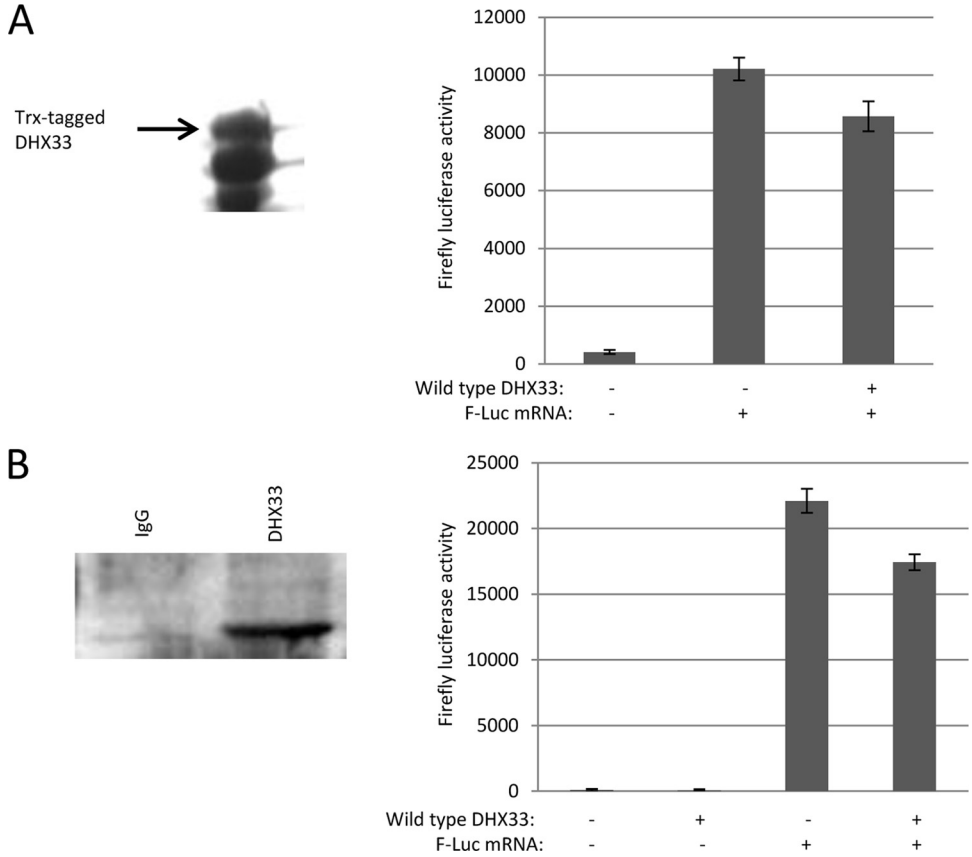

FIG 10 Purified DHX33 does not enhance luciferase mRNA translation *in vitro*. (A) The open reading frame of mouse DHX33 was cloned into the BamHI/HindIII sites in the pET32M-3C vector. The following primers were used to amplify DHX33 PCR products: forward primer 5′-ATTATAGGATCCATGCCGGAGGAGGCGAGCCT-3′ and reverse primer 5′-ATAAATAAGCTTGTTTCTGGCCGTTCTCAGCTT-3′. Overexpressed wild-type recombinant DHX33 with a thioredoxin (Trx) tag at its N terminus and a 6× His tag at its C terminus was affinity purified from *E. coli* through an Ni-nitrilotriacetic acid column (Qiagen). (Left) Coomassie blue-stained proteins showing the purity of crude DHX33, which was further verified by Western blotting. Approximately 0.5 μg of this DHX33 recombinant protein was added into a rabbit reticulocyte lysate system (catalog no. L4960; Promega) to monitor *in vitro* protein translation activity with firefly luciferase mRNA as a control. (Right) After DHX33 was added, protein translational activity was decreased slightly. (B) FLAG-tagged DHX33 overexpressed in HeLa cells was immunoprecipitated by anti-FLAG beads and was then added into a rabbit reticulocyte system (catalog no. L4960; Promega) to assay *in vitro* protein translation activity. (Left) The DHX33 protein was immunoprecipitated from the cell lysates by Western blotting; (right) the addition of wild-type DHX33 inhibits luciferase mRNA translation in this experimental setting.

35% of GAPDH was associated with heavy polysomes (fractions 19 and 20). Knockdown of DHX33 reduced the amount of GAPDH mRNA in the heavy polysomes (fractions 18 to 20) (Fig. 9E). The amount of GAPDH mRNA in the heavy fraction of cells infected with #2-shDHX33 was reduced 2-fold (Fig. 9F), while #4-shDHX33 (which had a better DHX33 knockdown efficiency than #2-shDHX33 [Fig. 9D]) nearly abolished all GAPDH mRNA (0.68%) in the heavy polysomes (Fig. 9F), with the GAPDH mRNA in cells infected with #4-shDHX33 instead showing a shift into the lighter polysomes (Fig. 9E, fractions 15 to 17). This result clearly indicates that the loss of DHX33 significantly reduces the translation of GAPDH. Notably, DHX33 deficiency also significantly increased the percentage of GAPDH mRNA on 80S monosomes from 0.68% to approximately 6 to 8% (Fig. 9G). Accumulation of GAPDH mRNA on 80S monosomes indicates a less efficient initiation of mRNA translation after the 80S subunit has been assembled.

To determine whether DHX33 silencing inhibits the translation of mRNAs with structured 5′ UTRs differently, we analyzed the polysome distribution for DDX5 mRNA after DHX33 knockdown. The 5′ UTR of DDX5 mRNA has 247 nucleotides and is much longer than the GAPDH 5′ UTR. The results shown in Fig. 9H to J demonstrate that DDX5 mRNA is more readily shifted from the heavy polysome fraction (from 83% down to 0%) into the light polysome fraction and monoribosomes, and the percentage of DDX5 mRNA associated with 80S monoribosome could be increased from 0% up to approximately 54% (for cells infected with #4-shDHX33). These results suggest that DHX33 knockdown has a more dramatic effect on structured mRNAs and implies that DHX33 knockdown leads to significant stalling, albeit not a complete blockade, of 80S ribosome complexes on mRNAs.

Purified DHX33 does not stimulate firefly luciferase mRNA *in vitro*. To study whether DHX33 stimulates protein translation *in vitro*, we purified recombinant DHX33 protein in *Escherichia coli* and transfected wild-type immunoprecipitated DHX33 into cells. However, in both cases, with the rabbit reticulocyte system, we could not detect DHX33-enhanced mRNA translation; rather, the addition of either recombinant DHX33 or immunoprecipitated DHX33 slightly inhibited mRNA translation (as shown in Fig. 10). We think that, on the one hand, it may still be difficult to

copy the complex *in vivo* situation for now, as we have limited knowledge of its detailed mechanism; on the other hand, the simple firefly luciferase mRNA plus rabbit reticulocyte system might not be a good system for us to detect the translational efficiency. A more straightforward analysis and more biochemical studies are needed in order to address this issue.

DISCUSSION

We have identified a new DEAH box RNA helicase, DHX33, involved in mRNA translation. This extends the list of RNA helicases involved in translation initiation; the previous list included eIF4A, DDX3, and DHX29 (16, 27). The activity of eIF4A and DHX29 helicases in the unwinding of mRNA 5′ UTRs is important to promote translation initiation, while the function of DDX3 in translation has been shown to be quite diverse. DDX3 is involved in promotion of the 80S ribosome and resolution of the eIF4/mRNA complex (28–31). Our findings now support a role for DHX33 to promote the assembly of an elongation-competent 80S ribosome at a late stage of translation initiation. As such, DHX33 likely participates in resolving the final translation initiation complex and primes it for elongation.

We have previously shown that nucleolar DHX33 promotes ribosome RNA synthesis (20), thus complicating the effect of DHX33 knockdown on mRNA translation. The difficulty often encountered in deciphering the function of DEAD box RNA helicases resides in their multitude of subcellular locations. To address this concern in our studies of DHX33, we successfully separated the nucleolar DHX33 function from the cytosolic function through the use of targeted DHX33 domain mutants. The DHX33 D1 mutant was largely confined to the cytosol and as such was unable to rescue the nucleolar rRNA transcription properties of DHX33. However, this mutant was fully capable of rescuing mRNA translation in the cytosol, thus separating these two functions of DHX33. The results of the heterokaryon shuttling assays reinforce these findings, clearly demonstrating that DHX33 mobilization throughout the cell is a dynamic process. This allows DHX33 to function in various cellular processes that take place in distinct subcellular locations.

Indeed, the cytosolic function of DHX33 in translation initiation occurs even in the face of diminished rRNA production in the nucleolus, separating the two processes. Our results indicate an elevation in the amounts of cytosolic ribosome subunits and 80S monosomes concomitantly with a loss of polysomes, even in the face of severe defects in nucleolar ribosome production in these cells (20). This is most likely due to the enormous stability of existing cytosolic ribosomes at the times where we assayed cytosolic polysome formation. Our results show that although there is an increase in the amount of cytosolic 80S ribosome due to DHX33 deficiency, the extent of the increase in the amount of the 80S ribosome is not as significant as that seen with other typical RNA helicases involved in translation initiation (32). This might be due to lower levels of rRNA production in the absence of DHX33 (20), making the moderate increase in 80S ribosome levels a result of a combination of both a reduction in the amount of rRNA and inhibition of translation initiation. Although the levels of cytosolic 80S ribosomes were increased by DHX33 deficiency, these ribosomes were not elongation competent. This implies that DHX33 must have some essential role in promoting mRNA translation. In agreement with this, we further demonstrated the association of DHX33 with the translation machinery and mRNAs. Furthermore, additional evidence from studies with nonstructured and structured mRNAs showed a failure of mRNA translation initiation, despite sufficient 80S monosome assembly, underscoring the role of DHX33 in the later stage of mRNA translation initiation.

The effect of the DHX33 loss on mRNA translation appears to be global and not necessarily selective for any specific mRNAs. However, it will be worthwhile to further characterize the pattern of mRNAs bound to DHX33 through further RNA interaction studies and subsequent deep sequencing. We had initially identified DHX33 to be a target downstream of mTOR activity. TOR has been shown to control both cap-dependent and terminal oligopyrimidine (TOP)-dependent mRNA translation (33). Our findings place DHX33 squarely downstream of mTOR to control global mRNA translation through translation initiation. While we found that many mRNAs were bound to DHX33 complexes, it is worth noting that the fold enhancement in their interaction varied greatly, highlighting the possibility that DHX33 directs a more selective translation initiation program, one that could be driven by mTOR signals.

ACKNOWLEDGMENTS

We thank the members of the J. Weber lab for their technical input and suggestions and the staff in the Department of Biology at the South University of Science and Technology of China who provided support to allow the experiments to be completed. We also thank the RNAi Consortium, the Children's Discovery Institute, and The Genome Institute at Washington University for providing lentiviral knockdown constructs.

This work was partially supported by U.S. NIH grant 1 R01CA120436 (to J. Weber), U.S. Department of Defense Era of Hope Scholar Award BC075004 (to J. Weber), and start-up funding from the South University of Science and Technology of China (to Y. Zhang).

We declare that we have no competing financial interests.

REFERENCES

1. **Jackson RJ, Hellen CU, Pestova TV.** 2010. The mechanism of eukaryotic translation initiation and principles of its regulation. Nat Rev Mol Cell Biol **11:**113–127. http://dx.doi.org/10.1038/nrm2838.
2. **Sonenberg N, Hinnebusch AG.** 2009. Regulation of translation initiation in eukaryotes: mechanisms and biological targets. Cell **136:**731–745. http://dx.doi.org/10.1016/j.cell.2009.01.042.
3. **Di Prisco GV, Huang W, Buffington SA, Hsu CC, Bonnen PE, Placzek AN, Sidrauski C, Krnjevic K, Kaufman RJ, Walter P, Costa-Mattioli M.** 2014. Translational control of mGluR-dependent long-term depression and object-place learning by eIF2alpha. Nat Neurosci **17:**1073–1082. http://dx.doi.org/10.1038/nn.3754.
4. **Scheper GC, van der Knaap MS, Proud CG.** 2007. Translation matters: protein synthesis defects in inherited disease. Nat Rev Genet **8:**711–723. http://dx.doi.org/10.1038/nrg2142.
5. **Signer RA, Magee JA, Salic A, Morrison SJ.** 2014. Haematopoietic stem cells require a highly regulated protein synthesis rate. Nature **509:**49–54. http://dx.doi.org/10.1038/nature13035.
6. **Zalfa F, Giorgi M, Primerano B, Moro A, Di Penta A, Reis S, Oostra B, Bagni C.** 2003. The fragile X syndrome protein FMRP associates with BC1 RNA and regulates the translation of specific mRNAs at synapses. Cell **112:**317–327. http://dx.doi.org/10.1016/S0092-8674(03)00079-5.
7. **Boussemart L, Malka-Mahieu H, Girault I, Allard D, Hemmingsson O, Tomasic G, Thomas M, Basmadjian C, Ribeiro N, Thuaud F, Mateus C, Routier E, Kamsu-Kom N, Agoussi S, Eggermont AM, Désaubry L, Robert C, Vagner S.** 2014. eIF4F is a nexus of resistance to anti-BRAF and anti-MEK cancer therapies. Nature **513:**105–109. http://dx.doi.org/10.1038/nature13572.
8. **Hsieh AC, Liu Y, Edlind MP, Ingolia NT, Janes MR, Sher A, Shi EY, Stumpf CR, Christensen C, Bonham MJ, Wang S, Ren P, Martin M, Jessen K, Feldman ME, Weissman JS, Shokat KM, Rommel C, Ruggero D.** 2012. The translational landscape of mTOR signalling steers cancer

initiation and metastasis. Nature **485:**55–61. http://dx.doi.org/10.1038/nature10912.
9. **Ruggero D.** 2013. Translational control in cancer etiology. Cold Spring Harb Perspect Biol **5:**a012336. http://dx.doi.org/10.1101/cshperspect.a012336.
10. **Iizuka N, Najita L, Franzusoff A, Sarnow P.** 1994. Cap-dependent and cap-independent translation by internal initiation of mRNAs in cell extracts prepared from Saccharomyces cerevisiae. Mol Cell Biol **14:**7322–7330.
11. **Kahvejian A, Svitkin YV, Sukarieh R, M'Boutchou MN, Sonenberg N.** 2005. Mammalian poly(A)-binding protein is a eukaryotic translation initiation factor, which acts via multiple mechanisms. Genes Dev **19:**104–113. http://dx.doi.org/10.1101/gad.1262905.
12. **Morino S, Imataka H, Svitkin YV, Pestova TV, Sonenberg N.** 2000. Eukaryotic translation initiation factor 4E (eIF4E) binding site and the middle one-third of eIF4GI constitute the core domain for cap-dependent translation, and the C-terminal one-third functions as a modulatory region. Mol Cell Biol **20:**468–477. http://dx.doi.org/10.1128/MCB.20.2.468-477.2000.
13. **Hinnebusch AG.** 2014. The scanning mechanism of eukaryotic translation initiation. Annu Rev Biochem **83:**779–812. http://dx.doi.org/10.1146/annurev-biochem-060713-035802.
14. **Das S, Maitra U.** 2001. Functional significance and mechanism of eIF5-promoted GTP hydrolysis in eukaryotic translation initiation. Prog Nucleic Acid Res Mol Biol **70:**207–231.
15. **Marintchev A.** 2013. Roles of helicases in translation initiation: a mechanistic view. Biochim Biophys Acta **1829:**799–809. http://dx.doi.org/10.1016/j.bbagrm.2013.01.005.
16. **Pisareva VP, Pisarev AV, Komar AA, Hellen CU, Pestova TV.** 2008. Translation initiation on mammalian mRNAs with structured 5′UTRs requires DExH-box protein DHX29. Cell **135:**1237–1250. http://dx.doi.org/10.1016/j.cell.2008.10.037.
17. **Tanner NK, Linder P.** 2001. DExD/H box RNA helicases: from generic motors to specific dissociation functions. Mol Cell **8:**251–262. http://dx.doi.org/10.1016/S1097-2765(01)00329-X.
18. **Liu Y, Lu N, Yuan B, Weng L, Wang F, Liu YJ, Zhang Z.** 2014. The interaction between the helicase DHX33 and IPS-1 as a novel pathway to sense double-stranded RNA and RNA viruses in myeloid dendritic cells. Cell Mol Immunol **11:**49–57. http://dx.doi.org/10.1038/cmi.2013.40.
19. **Mitoma H, Hanabuchi S, Kim T, Bao M, Zhang Z, Sugimoto N, Liu YJ.** 2013. The DHX33 RNA helicase senses cytosolic RNA and activates the NLRP3 inflammasome. Immunity **39:**123–135. http://dx.doi.org/10.1016/j.immuni.2013.07.001.
20. **Zhang Y, Forys JT, Miceli AP, Gwinn AS, Weber JD.** 2011. Identification of DHX33 as a mediator of rRNA synthesis and cell growth. Mol Cell Biol **31:**4676–4691. http://dx.doi.org/10.1128/MCB.05832-11.
21. **Zhang Y, Saporita AJ, Weber JD.** 2013. P19ARF and RasV(1)(2) offer opposing regulation of DHX33 translation to dictate tumor cell fate. Mol Cell Biol **33:**1594–1607. http://dx.doi.org/10.1128/MCB.01220-12.
22. **King JB, Gross J, Lovly CM, Rohrs H, Piwnica-Worms H, Townsend RR.** 2006. Accurate mass-driven analysis for the characterization of protein phosphorylation. Study of the human Chk2 protein kinase. Anal Chem **78:**2171–2181.
23. **Liu R, Iadevaia V, Averous J, Taylor PM, Zhang Z, Proud CG.** 2014. Impairing the production of ribosomal RNA activates mammalian target of rapamycin complex 1 signalling and downstream translation factors. Nucleic Acids Res **42:**5083–5096. http://dx.doi.org/10.1093/nar/gku130.
24. **Sydorskyy Y, Dilworth DJ, Halloran B, Yi EC, Makhnevych T, Wozniak RW, Aitchison JD.** 2005. Nop53p is a novel nucleolar 60S ribosomal subunit biogenesis protein. Biochem J **388:**819–826. http://dx.doi.org/10.1042/BJ20041297.
25. **Legrier ME, Yang CP, Yan HG, Lopez-Barcons L, Keller SM, Perez-Soler R, Horwitz SB, McDaid HM.** 2007. Targeting protein translation in human non small cell lung cancer via combined MEK and mammalian target of rapamycin suppression. Cancer Res **67:**11300–11308. http://dx.doi.org/10.1158/0008-5472.CAN-07-0702.
26. **Lin CJ, Robert F, Sukarieh R, Michnick S, Pelletier J.** 2010. The antidepressant sertraline inhibits translation initiation by curtailing mammalian target of rapamycin signaling. Cancer Res **70:**3199–3208. http://dx.doi.org/10.1158/0008-5472.CAN-09-4072.
27. **Chuang RY, Weaver PL, Liu Z, Chang TH.** 1997. Requirement of the DEAD-box protein Ded1p for messenger RNA translation. Science **275:**1468–1471. http://dx.doi.org/10.1126/science.275.5305.1468.
28. **Geissler R, Golbik RP, Behrens SE.** 2012. The DEAD-box helicase DDX3 supports the assembly of functional 80S ribosomes. Nucleic Acids Res **40:**4998–5011. http://dx.doi.org/10.1093/nar/gks070.
29. **Harms U, Andreou AZ, Gubaev A, Klostermeier D.** 2014. eIF4B, eIF4G and RNA regulate eIF4A activity in translation initiation by modulating the eIF4A conformational cycle. Nucleic Acids Res **42:**7911–7922. http://dx.doi.org/10.1093/nar/gku440.
30. **Lee CS, Dias AP, Jedrychowski M, Patel AH, Hsu JL, Reed R.** 2008. Human DDX3 functions in translation and interacts with the translation initiation factor eIF3. Nucleic Acids Res **36:**4708–4718. http://dx.doi.org/10.1093/nar/gkn454.
31. **Soto-Rifo R, Rubilar PS, Limousin T, de Breyne S, Decimo D, Ohlmann T.** 2012. DEAD-box protein DDX3 associates with eIF4F to promote translation of selected mRNAs. EMBO J **31:**3745–3756. http://dx.doi.org/10.1038/emboj.2012.220.
32. **Parsyan A, Shahbazian D, Martineau Y, Petroulakis E, Alain T, Larsson O, Mathonnet G, Tettweiler G, Hellen CU, Pestova TV, Svitkin YV, Sonenberg N.** 2009. The helicase protein DHX29 promotes translation initiation, cell proliferation, and tumorigenesis. Proc Natl Acad Sci U S A **106:**22217–22222. http://dx.doi.org/10.1073/pnas.0909773106.
33. **Thoreen CC, Chantranupong L, Keys HR, Wang T, Gray NS, Sabatini DM.** 2012. A unifying model for mTORC1-mediated regulation of mRNA translation. Nature **485:**109–113. http://dx.doi.org/10.1038/nature11083.